Preprints (www.preprints.org) | NOT PEER-REVIEWED | Posted: 31 March 2022 doi:10.20944/preprints202203.0409.v1

Title: Comparison of laminoplasty on lordotic, straight and kyphotic cervical alignments suggest poor outcomes for kyphotic cervical alignment: finite element analysis.

Norihiro Nishida, MD. PhD,[1] , Muzammil Mumtaz,[2] Sudharshan Tripathi,[2] Amey Kelkar,[2] Mendoza Justin,[2] Yogesh Kumaran,[2] and Vijay K. Goel, PhD[2]

[1] Department of Orthopedic Surgery, Yamaguchi University Graduate School of Medicine, 1-1-1 Minami-Kogushi, Ube City, Yamaguchi Prefecture 755-8505, Japan; telephone: 81-836-22-2268; fax: 81-836-22-2267

[2] Engineering Center for Orthopaedic Research Excellence (E-CORE), Departments of Bioengineering and Orthopaedics, The University of Toledo, Toledo, Ohio.; telephone: 1-(419) 530- 8035; fax: (419) 530-8076

Ethical statement

This study was approved from the ethical review board of the Toledo Medical Center (No. 500058).

Conflict of interest: No benefits in any form have been received or will be acquired by a commercial party related directly or indirectly to the subject of this article.

Contact information

1. **Corresponding Author:** Norihiro Nishida; Department of Orthopedic Surgery, Yamaguchi University Graduate School of Medicine, 1-1-1 Minami-Kogushi, Ube City, Yamaguchi Prefecture 755-8505, Japan; telephone: 81-836-22-2268; fax: 81-836-22-2267; e-mail; nishida3@yamaguchi-u.ac.jp
2. Muzammil Mumtaz: Engineering Center for Orthopaedic Research Excellence (E-CORE), Departments of Bioengineering and Orthopaedics, The University of Toledo, Toledo, Ohio.; telephone: 1- (419) 530- 8035; fax: (419) 530-8076; e-mail: Muzammil.Mumtaz@rockets.utoledo.edu
3. Sudharshan Tripathi: Engineering Center for Orthopaedic Research Excellence (E-CORE), Departments of Bioengineering and Orthopaedics, The University of Toledo, Toledo, Ohio.; telephone: 1- (419) 530- 8035; fax: (419) 530-8076; e-mail: Sudharshan.Tripathi@rockets.utoledo.edu

4. Amey Kelkar: Engineering Center for Orthopaedic Research Excellence (E-CORE), Departments of Bioengineering and Orthopaedics, The University of Toledo, Toledo, Ohio.; telephone: 1- (419) 530- 8035; fax: (419) 530-8076; email: Amey.Kelkar@rockets.utoledo.edu

5. Mendoza Justin: Engineering Center for Orthopaedic Research Excellence (E-CORE), Departments of Bioengineering and Orthopaedics, The University of Toledo, Toledo, Ohio.; telephone: 1- (419) 530- 8035; fax: (419) 530-8076; email: Justin.Mendoza@rockets.utoledo.edu
6. Yogesh Kumaran: Engineering Center for Orthopaedic Research Excellence (E-CORE), Departments of Bioengineering and Orthopaedics, The University of Toledo, Toledo, Ohio.; telephone: 1- (419) 530- 8035; fax: (419) 530-8076; email: yogesh.kumaran@rockets.utoledo.edu
7. Vijay K. Goel: Engineering Center for Orthopaedic Research Excellence (E-CORE), Departments of Bioengineering and Orthopaedics, The University of Toledo, 2801 West Bancroft Street, MS 303, NI Hall, Room 5046, Toledo, OH 43606; telephone: 1- (419) 530- 8035; fax: (419) 530-8076; email: Vijay.Goel@utoledo.edu

 doi:10.20944/preprints202203.0409.v1

Abstract

Background: Cervical laminoplasty is a useful for treatment of cervical myelopathy. However, this procedure has limitations for kyphotic cervical alignments. We used the finite element (FE) analysis and investigated the biomechanical changes in an intact and laminoplasty models with lordosis, straight, and kyphosis cervical alignments.

Methods: A three-dimensional FE model of the cervical spine (C2-C7) with ligaments was created from computed tomography. The model was modified with the following cobb angles and the C3-C6 laminoplasty was conducted; a) laminoplasty-lordotic model (LM-L; C2-C7 angle: -10°), b) laminoplasty-straight model (LM-S; C2-C7 angle: 0°), and c) laminoplasty-kyphotic model (LM-K; C2-C7 angle: 10°). A pure moment with a compressive follower load of 100N to represent the weight of the head/cranium and cervical muscle stabilization was applied to these models. The range of motion (ROM), annular stress, nucleus stress and facet forces were analyzed.

Results: ROM of LM-K increased when compared to the other models except for flexion. The LM-K had the highest mobility with 49% increase in ROM observed under extension, compared to the intact model. In all motion except for flexion, LM-L models' ROM decreased by more than 10%, and LM-S and LM-K models' ROM increased by more than 10% at C2-C7 compared to the intact model. The annular stresses and nucleus stresses in LM-K were higher compared to the other models. The maximum increase in annular stresses was about 194% in LM-K compared to the intact model, observed at the C3-C4 segment. The facet contact forces were lowest in the LM-K, compared to the other models.

Conclusions: Patients with a cervical kyphosis alignment are at a disadvantage of increased kyphosis compared to cases with lordosis or straight alignment and should be treated with caution.

Keywords: cervical alignment; cervical laminoplasty; spinal cord; finite element analysis; cervical spine biomechanics

 doi:10.20944/preprints202203.0409.v1

Introduction

In cervical spondylotic myelopathy (CSM), cervical disc herniation (CDH), and cervical ossification of the posterior longitudinal ligament (C-OPLL), asymptomatic patients with radiculopathy or myelopathy may be considered for surgical decompression [1]. Laminoplasty is a decompression procedure of the lamina for the spinal cord with positive surgical outcomes and improved techniques [2]. Although anterior decompression and fixation is also an important technique for decompression of the spinal cord, laminoplasty is often chosen because it allows for a wider decompression range and is relatively easy to perform [3,4]. However, complications such as increased kyphosis and axial pain may occur more often after conducting laminoplasty compared to anterior decompression and fixation because laminoplasty invades the cervical posterior ligament complex which can disturb the cervical sagittal balance[5]. Specifically, laminoplasty for straight or kyphotic curvatures of the cervical spine is not recommended because the laminoplasty may not create enough posterior migration or may cause impingement, stretch injury of the spinal cord, postoperative kyphotic deformity, and loss of range of motion (ROM)[6,7].

There are no reports that have examined the extent to which the ROM of the cervical spine, stresses on the intervertebral discs and facet joint contact biomechanics change when the laminoplasty procedure is performed for different alignments. We examined the biomechanical changes on the when double-door laminoplasty [8] is performed on cervical spines with lordosis, straight, and kyphosis alignments. We hypothesized that the ROM, stress contribution of the disc, intervertebral body, and facet loads may change for the cervical alignment if the same laminoplasty was conducted. This study would provide mechanically important information for a physician performing laminoplasty and whether additional anterior decompression and fixation or posterior fixation with instrumentation is necessary, depending on the cervical spine alignment.

In this study, a C2-C7 three-dimension (3D) FE model of a cervical spine with three alignments (lordosis, straight, and kyphosis) were created to examine how stress and mobility in the cervical spine changed for different alignments post double-door laminoplasty surgery.

Material and methods

Model Development

A validated FE model of the cervical spine (C2-C7) was used in this study [9]. In summary, the FE model was created based on the computed tomography (CT) images of an adult subject. This study was approved from the ethical review board of the Toledo Medical Center (No. 500058). The three-dimensional reconstruction of the cervical spine geometry (vertebrae as well as intervertebral discs) from CT scans was carried out using the image segmentation software MIMICS v 15.0 (Materialise, Leuven, Belgium). The reconstructed geometry of hard and soft tissues was meshed with the hexahedral elements using IA-FE MESH software (Iowa, United States). The meshed vertebrae/discs were exported to ABAQUS software (Dassault Systèmes, Simulia Inc., Providence, RI) to assemble the C2-C7 cervical spine. The anterior Longitudinal Ligament (ALL), posterior Longitudinal

 doi:10.20944/preprints202203.0409.v1

Ligament (PLL), interspinous ligament (ISL), supraspinous ligament (SSL), capsular ligament (CL), ligamentum flavum (LF) using truss elements in ABAQUS were added to the model[11]. The outer 0.5mm layer of vertebrae represented cortical shell, and the inside represented cancellous bone[12]. The intervertebral discs were composed of annulus fibrosus (50%) and nucleus pulposus (50%). The annulus consisted of ground substance along with embedded fibers oriented at ±25° [10]. The facet joints in the model were represented using surface-surface sliding contact, whereas the Lushka's joints in the lower cervical intervertebral discs were modeled using GAPUNI elements. The material properties for all the structures in the FE model were taken from the literature and are summarized in Table 1[13-15]. This was set as intact model.

Cervical Alignments

Cobb angles were used as cervical spine parameters [16]. A lateral radiograph showing Cobb angle (C2-C7 angle) measurements were utilized using the 4-line method described by Harrison et al [17]. The 4-line method involves: drawing a line parallel from the inferior endplate of C2 to the posterior margin of the spinous process with another line parallel to the inferior endplate of C7. Then, perpendicular lines are drawn from each of the 2 lines noted above and the angle subtended between the crossings of the perpendicular lines is the cervical curvature angle. The cervical sagittal balance is as follows: the spino-cranial angle (SCA) (angle between the C7 slope and the straight line joining the middle of the C7 end plate and the middle of the sella turcica), and the cervical sagittal vertical axis

Preprints (www.preprints.org) | NOT PEER-REVIEWED | Posted: 31 March 2022 doi:10.20944/preprints202203.0409.v1

(cSVA), (cSVA is the distance from a vertical plumb line dropped from the center of the C2 vertebral body to the posterior superior corner of the C7 vertebra). The intact model used for cervical validation had a C2-C7 lordosis with a cobb angle of -5°. The intact model was modified, and the three different alignments models were created by iteratively applying displacements/rotations to cervical vertebrae until the desired alignment parameter was obtained. For example, for creating a kyphotic model, the C7 vertebra was fixed and rotation at C2 was applied until C2-C7=10°(kyphosis) was obtained. By modification, the following were created a) intact-lordotic model (intact-L; C2-C7 angle : -10°, cSVA: 25mm, the C7 slope: 20°), b) intact-straight model (intact-S; C2-C7 angle : 0°, cSVA: 31mm, the C7 slope: 22°), and c) intact-kyphotic model (intact-K; C2-C7 angle : 10°, cSVA: 38mm, the C7 slope: 24°) (Figure 1 A-C).

Cervical Laminoplasty

Double door laminoplasty was simulated on the three intact models by performing osteotomy at the central spinous process and lamina. First, the ISL and SSL were resected. Next, the spinous process was partially resected. About 4mm of bone from the center of the lamina was cut, and the medial side of both the facet joints was shaved so that lamina could be opened (Figure 1D, E). The LF of C2-C3 and C6-C7 was excised because these interfered with the opening of the lamina which was opened to the right and left sides (Figure 1F). Moreover, it widened the narrow canal and simulated the decompression of the spinal cord posteriorly. The artificial bone with 4 mm height and

 doi:10.20944/preprints202203.0409.v1

8 mm depth was then placed to fit into the opened lamina (Figure 1F). The artificial bones were attached to the either side of the lamina via “TIE” constraint formulation in ABAQUS to represent firm attachment of bone graft to the lamina. The material properties of the artificial bone were the same as the cortical bone. The same procedure was used to create a double-door laminoplasty model of C3-C6, in which the lamina and the artificial bone were set to be connected in all directions (Figure 1F). The C3-C6 double door laminoplasty using this methodology was conducted on the intact-lordosis, intact-straight, and intact-kyphosis configurations. The resulting laminoplasty models were represented by laminoplasty-lordosis model (LM-L), laminoplasty-straight model (LM-S), and laminoplasty-kyphosis model (LM-K).

Loads and Boundary Conditions

A pure moment of 1.5 Nm was applied to the C2 odontoid process to simulate six motions to flexion/extension, lateral (left and right) bending, axial (left and right) rotations, and the inferior endplate of the C7 was fixed. The model was subjected to the compressive follower load of 100N to represent the weight of the head/cranium and cervical muscle stabilization[18].

Data Analyses

The ROM, annular stresses, intradiscal (nucleus) stresses, and facet contact forces were calculated for intact, LM-L, LM-S, and LM-K. Annular stresses and nucleus stresses were noted by the maximum von Mises stress. For the facet joint force, the data for facet forces were averaged for the left/right facets. The percentage change (%) was calculated using the following equation:

$$Percentage\ change\ (\%) = \frac{Intac\ \ Model\ Data - Laminoplasty\ Model\ Data}{Intact\ Model\ Data} * 100$$

Results

ROM

In extension, LM-L models' ROM decreased by 35%, and LM-S and LM-K models' ROM increased by 28% and 49% at C2-C7 compared to the intact model. In flexion, LM-L model's ROM increased by 3%, and LM-S and LM-K model's ROM decreased at C2-C3, C3-C4, C4-C5, and C2-C7 compared to the intact model. In left bending, LM-L model's ROM decreased by 20%, and LM-S and LM-K model's ROM increased by 15% and 26% at C2-C7 compared to the intact model. In right bending, LM-L model's ROM decreased by 13%, and LM-S and LM-K model's ROM increased by 10% and 15% at C2-C7 compared to the intact model. In left rotation, LM-L model's ROM decreased by 16%, and LM-S and LM-K model's ROM increased by 10% and 16% at C2-C7 compared to the intact model. In right rotation, LM-L model's ROM decreased by 15%, and LM-S and LM-K model's ROM increased by 8% and 15% at C2-C7 compared to the intact model (Figure 2).

Annular stress

In extension, the annular stresses decreased by 37%, 39%, and 21% at C2-C3, C3-C4, and C4-C5 in

 doi:10.20944/preprints202203.0409.v1

the LM-L when compared to the intact model. The annular stresses increased by 18%, 23%, and 11% at C3-C4, C4-C5, and C5-C6 in the LM-S and by 24%, 59%, and 80% at C3-C4, C4-C5, and C5-C6 in the LM-K when compared to the intact model. In flexion, the annular stresses decreased by 23% at C3-C4 in the LM-L when compared to the intact model. The annular stresses increased by 55% at C3-C4 in the LM-S and by 71% at C3-C4 in the LM-K when compared to the intact model. In left bending, the annular stresses decreased by 16% at C3-C4 in the LM-L when compared to the intact model. The annular stresses increased by 108% at C3-C4 in the LM-S and by 194% at C3-C4 in the LM-K when compared to the intact model. In right bending, the annular stresses decreased by 34% at C3-C4 in the LM-L when compared to the intact model. The annular stresses increased by 24% at C3-C4 in the LM-S and by 48% at C3-C4 in the LM-K when compared to the intact model. In left rotation, the annular stresses decreased by 27% in the LM-L and by 9% at C3-C4 in the LM-S when compared to the intact model. The annular stresses increased by 24% at C3-C4 in the LM-K when compared to the intact model. In right rotation, the annular stresses decreased by 16% at C3-C4 in the LM-L when compared to the intact model. The annular stresses increased by 18% at C3-C4 in the LM-S and by 69% at C3-C4 in the LM-K when compared to the intact model (Figure 3).

Nucleus stresses

In extension, the nucleus stresses decreased in the LM-L model, LM-S and LM-K model compared to the intact model in all levels. For flexion, nucleus stresses increased in LM-L model in comparison

 doi:10.20944/preprints202203.0409.v1

with the LM-S and LM-K. In left bending, the nucleus stresses increased in the LM-K compared to the LM-L and LM-S models except for C2-C3. In right bending, higher nucleus stresses were observed at all levels for the LM-K compared to the intact, LM-L and LM-S model. In left and right axial rotation, the nucleus stress was increased in the LM-K model when compared to the intact model, LM-L and LM-S models (Figure 4).

Facet contact forces

In extension, the facet contact forces at all levels for LM-L increased by 20-60% respectively compared to the intact model. the facet contact forces at all levels for LM-S and LM-K decreased by 30-45% and 58-95% respectively compared to the intact model. In lateral bending, the facet contact forces at all levels for LM-L increased by 15-27% respectively compared to the intact model. The facet contact forces at all levels for LM-S and LM-K decreased by 10-46% and 19-57% respectively compared to the intact model. In rotation, the facet contact forces at all levels for LM-L increased by 14-89% respectively compared to the intact model. The facet contact forces at all levels except for C2-C3 for LM-S decreased by 24-45% respectively compared to the intact model. The facet contact forces at all levels for LM-K decreased by 43-90% respectively compared to the intact model (Figure 5).

 doi:10.20944/preprints202203.0409.v1

Discussion

This study aimed to investigate the biomechanical changes for lordotic, straight, and kyphotic cervical sagittal alignments models following cervical laminoplasty.

The cervical spine is an important part of the body that supports the head and provides sufficient mobility and protection to the cervical spinal cord, but once neurological symptoms occur, anterior or posterior decompression (laminectomy or laminoplasty) may be required. Laminoplasty is usually reported to increase the stability of the cervical spine. Seichi et al. reported that mean mobility decreased from 36° to 8° following double door laminoplasty [19]. Additionally, Ratliff and Cooper reported that the ROM was reduced by 50% for double-door laminoplasty relative to pre-operation measurements [20]. The effect of cervical alignment on surgical intervention is debated. There are few reports on what Cobb angles are acceptable for cervical laminoplasty. Lee reported that the patients with straight or lordosis (range, 1°–14°) may also be suitable for laminoplasty [21]. In general, it has been reported that laminoplasty is not effective for patients with C-OPLL and having cervical spine kyphosis along with high cSVA[7,22]. The clinical review reported the ranges of two sagittal parameters for desired post-operative clinical outcomes: C7 slope, average value 20°, must not be higher than 40° and cSVA must be less than 40 mm (mean value 20 mm) [23]. In this analysis, for extension, both bending and both rotations, the LM-L model only showed decrease in ROM compared to other models. The ROM became higher as kyphosis increased. These results agree with reports in literature that claimed that complications such as increased kyphosis may occur after conducting laminoplasty for cases with kyphosis alignment [6,7]. The annulus stresses generally increased as the kyphosis increased. The largest differences for the annulus stresses between the intact and laminoplasty models were observed in C3-C4. This could be because the posterior ligaments were stretched as kyphosis increased, and the laminoplasty damaged the posterior ligaments, resulting in increased stress in the annulus. For nucleus stresses, lower stresses were observed for the LM-L model than the intact model in all motions except for left bending. The facet forces were the highest in the LM-L model, which may be due to the distance between the facet joints in that specific alignment. In this analysis, the spinous processes, lamina, and the artificial bones were also closer in the lordotic alignment, but they never came in contact during any motion. The facet forces in the LM-S model were higher than the intact model in flexion, bending, and rotation motions, especially in C2-C3, possibly due to stabilization by laminoplasty. Conversely, in kyphosis, there was a possibility that the load was further decreased by laminoplasty. The facet force was reduced in all motions, and the function of the facet joint can be weakened. The results of the ROM, annulus stresses, nucleus stresses and facet forces suggested that laminoplasty in cervical kyphosis alignments may result in negative clinical outcomes. On the other hand, Kim showed that patients having within 10° of cervical kyphosis had similar postoperative outcome compared to patients with normative cervical lordotic alignment following posterior decompression with laminoplasty [6]. Matsunaga reported successful neurologic outcomes for patients with up to 13 degrees of kyphosis after cervical laminoplasty [24]. Thus, the debate continues about sagittal alignment and posterior procedures, and it will be necessary to analyze

 doi:10.20944/preprints202203.0409.v1

a model with increased kyphosis angle in the future.

The published studies on the biomechanical effects of laminoplasty of the cervical spine can be largely divided into FE analysis and cadaver analysis studies. In FE analysis studies, reports of laminectomy are far more common than reports of laminoplasty [25]. We did not analyze laminectomy in this study. Hashiguchi reported the difference in stresses in the cervical spine after different laminoplasty surgeries including open door laminoplasty, French door laminoplasty, and double-door laminoplasty. They reported that laminoplasty was more stable than the intact model[26]. In our study, the results were similar only for LM-L. Kode reported that during flexion, the percent changes in C2-T1 ROM of LM resulted in 20% increase, and in left bending, a decrease of 20% was observed. Similarly, left axial rotation resulted in 15% decrease in motion at C6-C7 after double-door laminoplasty [27]. In our study, LM-L showed the same trend, however, previous reports didn’t consider the cervical alignment.

In cadaver analysis studies, Kubo reported three-dimensional kinematic changes after double-door cervical laminoplasty. They found that laminoplasty showed no significant differences in motion compared with intact except in axial rotation[28]. Subramaniam reported that open-door laminoplasty left the spine in a significantly more stable condition than laminectomy after comparing biomechanical stability during flexion and extension [29]. These results indicated the contribution of laminoplasty to stability. Our results also showed a similar trend for LM-L. To the best of our knowledge, our study is the first to examine various sagittal alignments on the cervical spine .

There are several limitations to our study. The models do not include muscles, though the effect of musculature was addressed by the follower load technique [17]. Additionally, the only cervical alignments analyzed were lordotic, straight, and kyphosis alignments. A model with increased kyphosis should also be explored. The current study also does not include a spinal cord or take osteoporosis or osteoarthritis into consideration which may alter the material properties of the bone. Kyphosis of the thoracic spine and total spine alignment were also not considered. This model simulates an immediate postoperative scenario and does not consider conditions such as fusion and non-fusion of the lamina. The study also does not fully simulate the long-term outcome of laminoplasty. Although there are several methods of laminoplasty [26], the current study only analyzes double-door laminoplasty. Despite these limitations, this study provides valuable insight on the biomechanical outcome of laminoplasty in different cervical sagittal alignments.

Conclusions

An FE model created from medical images was used to analyze laminoplasty for different cervical sagittal alignments (lordotic, straight, and kyphotic). The results of this study indicate that as the cervical alignment changes from lordotic to kyphotic; the ROM, annulus stress, and nucleus stress after laminoplasty tend to increase. In summary, cases with cervical kyphosis alignment are disadvantageous compared to a case with lordotic or straight alignments and should be treated with caution when considering laminoplasty.

References

1 Boody, B. S., Lendner, M. & Vaccaro, A. R. Ossification of the posterior longitudinal ligament in the cervical spine: a review. *Int Orthop* **43**, 797-805, doi:10.1007/s00264-018-4106-5 (2019).

2 Hirabayashi, S., Kitagawa, T., Yamamoto, I., Yamada, K. & Kawano, H. Development and Achievement of Cervical Laminoplasty and Related Studies on Cervical Myelopathy. *Spine Surg Relat Res* **4**, 8-17, doi:10.22603/ssrr.2019-0023 (2020).

3 Lee, N. J., Kim, J. S., Park, P. & Riew, K. D. A Comparison of Various Surgical Treatments for Degenerative Cervical Myelopathy: A Propensity Score Matched Analysis. *Global Spine J*, 2192568220976092, doi:10.1177/2192568220976092 (2020).

4 Yoshii, T. *et al.* A systematic review and meta-analysis comparing anterior decompression with fusion and posterior laminoplasty for cervical spondylotic myelopathy. *J Orthop Sci* **26**, 116-122, doi:10.1016/j.jos.2020.02.008 (2021).

5 Tang, J. A. *et al.* The impact of standing regional cervical sagittal alignment on outcomes in posterior cervical fusion surgery. *Neurosurgery* **76 Suppl 1**, S14-21; discussion S21, doi:10.1227/01.neu.0000462074.66077.2b (2015).

6 Kim, S. W. *et al.* Analysis of Cervical Spine Alignment and its Relationship with Other Spinopelvic Parameters After Laminoplasty in Patients with Degenerative Cervical Myelopathy. *J Clin Med* **9**, doi:10.3390/jcm9030713 (2020).

7 Machino, M. *et al.* Cervical alignment and range of motion after laminoplasty: radiographical data from more than 500 cases with cervical spondylotic myelopathy and a review of the literature. *Spine (Phila Pa 1976)* **37**, E1243-1250, doi:10.1097/BRS.0b013e3182659d3e (2012).

8 Kurokawa, R. & Kim, P. Cervical Laminoplasty: The History and the Future. *Neurol Med Chir (Tokyo)* **55**, 529-539, doi:10.2176/nmc.ra.2014-0387 (2015).

9 Nishida, N. *et al.* Biomechanical Analysis of Posterior Ligaments of Cervical Spine and Laminoplasty. *Applied Sciences* **11**, 7645 (2021).

10 Kallemeyn, N. *et al.* Validation of a C2-C7 cervical spine finite element model using specimen-specific flexibility data. *Med Eng Phys* **32**, 482-489, doi:10.1016/j.medengphy.2010.03.001 (2010).

11 Mumtaz, M.; Zafarparandeh, I.; Taherzadeh, P.; Akıncı, S.Z.; Erbulut, D.U. Effect of U-shaped implant on the biomechanics of the cervical spine. In Proceedings of the 2016 20th National Biomedical Engineering Meeting (BIYOMUT), Izmir, Turkey, 3–5 November 2016; pp. 1–3. doi: 10.1109/BIYOMUT.2016.7849374.

12 Mumtaz, M., Mendoza, J., Vosoughi, A. S., Unger, A. S., & Goel, V. K. (2021). A Comparative Biomechanical Analysis of Various Rod Configurations Following Anterior Column Realignment and Pedicle Subtraction Osteotomy. Neurospine,

18(3),587.doi:10.14245/ns.2142450.225

13 Finn, M. A., Brodke, D. S., Daubs, M., Patel, A. & Bachus, K. N. Local and global subaxial cervical spine biomechanics after single-level fusion or cervical arthroplasty. *Eur Spine J* 18, 1520-1527, doi:10.1007/s00586-009-1085-7 (2009).

14 Goel, V. K. & Clausen, J. D. Prediction of load sharing among spinal components of a C5-C6 motion segment using the finite element approach. *Spine (Phila Pa 1976)* 23, 684-691, doi:10.1097/00007632-199803150-00008 (1998).

15 Little, J. P., Adam, C. J., Evans, J. H., Pettet, G. J. & Pearcy, M. J. Nonlinear finite element analysis of anular lesions in the L4/5 intervertebral disc. *J Biomech* 40, 2744-2751, doi:10.1016/j.jbiomech.2007.01.007 (2007).

16 Ling, F. P. *et al.* Which parameters are relevant in sagittal balance analysis of the cervical spine? A literature review. *Eur Spine J* 27, 8-15, doi:10.1007/s00586-018-5462-y (2018).

17 Harrison, D. E. *et al.* Cobb method or Harrison posterior tangent method: which to choose for lateral cervical radiographic analysis. *Spine (Phila Pa 1976)* 25, 2072-2078, doi:10.1097/00007632-200008150-00011 (2000).

18 Patwardhan, A. G. *et al.* Effect of compressive follower preload on the flexion-extension response of the human lumbar spine. *J Orthop Res* 21, 540-546, doi:10.1016/s0736-0266(02)00202-4 (2003).

19 Seichi, A. *et al.* Long-term results of double-door laminoplasty for cervical stenotic myelopathy. *Spine (Phila Pa 1976)* 26, 479-487, doi:10.1097/00007632-200103010-00010 (2001).

20 Ratliff, J. K. & Cooper, P. R. Cervical laminoplasty: a critical review. *J Neurosurg* 98, 230-238, doi:10.3171/spi.2003.98.3.0230 (2003).

21 Lee, J. Y. *et al.* Quantitative prediction of spinal cord drift after cervical laminectomy and arthrodesis. *Spine (Phila Pa 1976)* 31, 1795-1798, doi:10.1097/01.brs.0000225992.26154.d0 (2006).

22 Inose, H. *et al.* Factors Negatively Influencing Postoperative Improvement After Laminoplasty in Degenerative Cervical Myelopathy. *Clin Spine Surg*, doi:10.1097/bsd.0000000000001207 (2021).

23 Azimi, P., Yazdanian, T., Benzel, E. C., Hai, Y. & Montazeri, A. Sagittal balance of the cervical spine: a systematic review and meta-analysis. *Eur Spine J*, doi:10.1007/s00586-021-06825-0 (2021).

24 Matsunaga, S., Sakou, T. & Nakanisi, K. Analysis of the cervical spine alignment following laminoplasty and laminectomy. *Spinal Cord* 37, 20-24, doi:10.1038/sj.sc.3100749 (1999).

25 Khuyagbaatar, B., Kim, K., Park, W. M., Lee, S. & Kim, Y. H. Increased stress and strain on the spinal cord due to ossification of the posterior longitudinal ligament in the cervical

 doi:10.20944/preprints202203.0409.v1

spine under flexion after laminectomy. *Proc Inst Mech Eng H* **231**, 898-906, doi:10.1177/0954411917718222 (2017).

26 Hashiguchi, A., Kanchiku, T., Nishida, N. & Taguchi, T. Biomechanical Study of Cervical Posterior Decompression. *Asian Spine J* **12**, 391-397, doi:10.4184/asj.2018.12.3.391 (2018).

27 Kode, S., Kallemeyn, N. A., Smucker, J. D., Fredericks, D. C. & Grosland, N. M. The effect of multi-level laminoplasty and laminectomy on the biomechanics of the cervical spine: a finite element study. *Iowa Orthop J* **34**, 150-157 (2014).

28 Kubo, S., Goel, V. K., Yang, S. J. & Tajima, N. The biomechanical effects of multilevel posterior foraminotomy and foraminotomy with double-door laminoplasty. *J Spinal Disord Tech* **15**, 477-485, doi:10.1097/00024720-200212000-00008 (2002).

29 Subramaniam, V. *et al.* Biomechanical effects of laminoplasty versus laminectomy: stenosis and stability. *Spine (Phila Pa 1976)* **34**, E573-578, doi:10.1097/BRS.0b013e3181aa0214 (2009).

Preprints (www.preprints.org) | NOT PEER-REVIEWED | Posted: 31 March 2022 doi:10.20944/preprints202203.0409.v1

Figure Legends

Figure 1. The intact (C2-C7) FE model. (A)Lordosis model. (B)Straight model. (C) Kyphosis model.

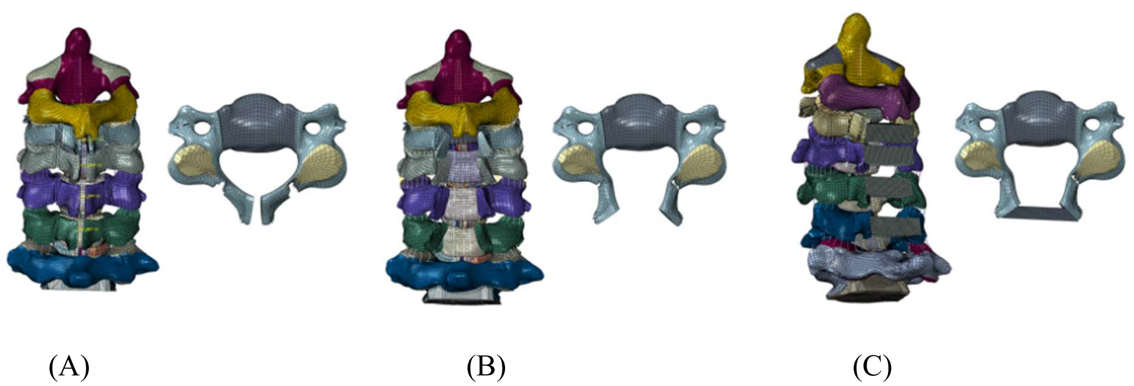

Figure 2. The laminoplasty model. (A) the spinous process was partially resected, about 4mm of bone from the center of the lamina was cut and the medial side of both the facet joints was shaved (C3-C6). (B) The lamina was opened to the lateral sides. (C) The laminoplasty model (C3-C6).

 doi:10.20944/preprints202203.0409.v1

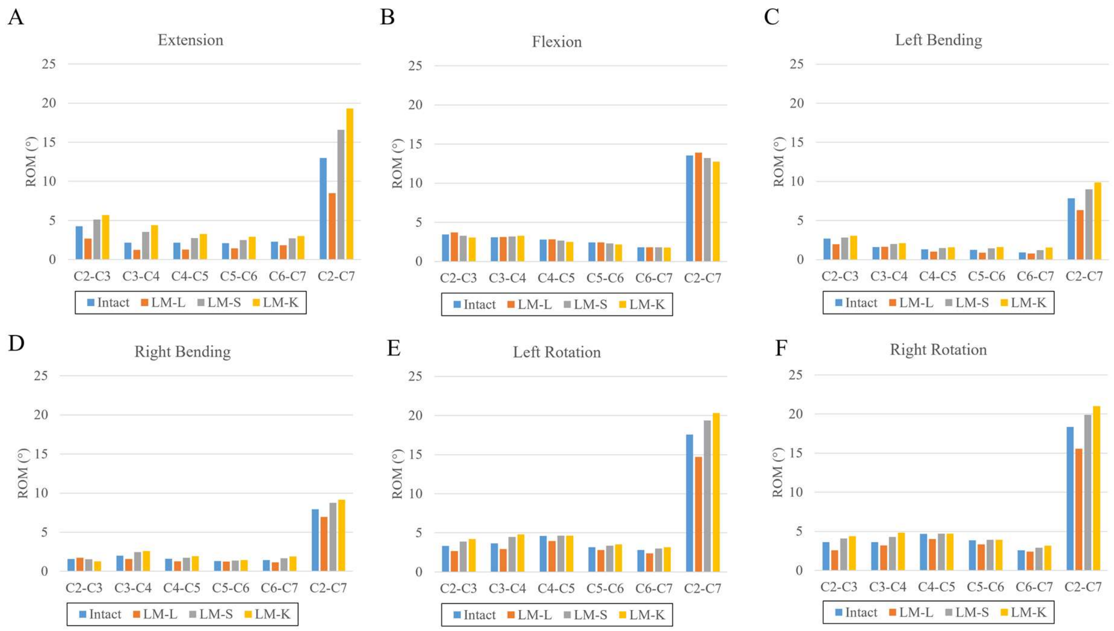

Figure 3. Range of motion. (a) extension, (b) flexion, (c) left bending, (d) right bending, (e) left rotation, and (f) right rotation. The vertical axis is an angle (degree), the horizontal axis is each intervertebral level.

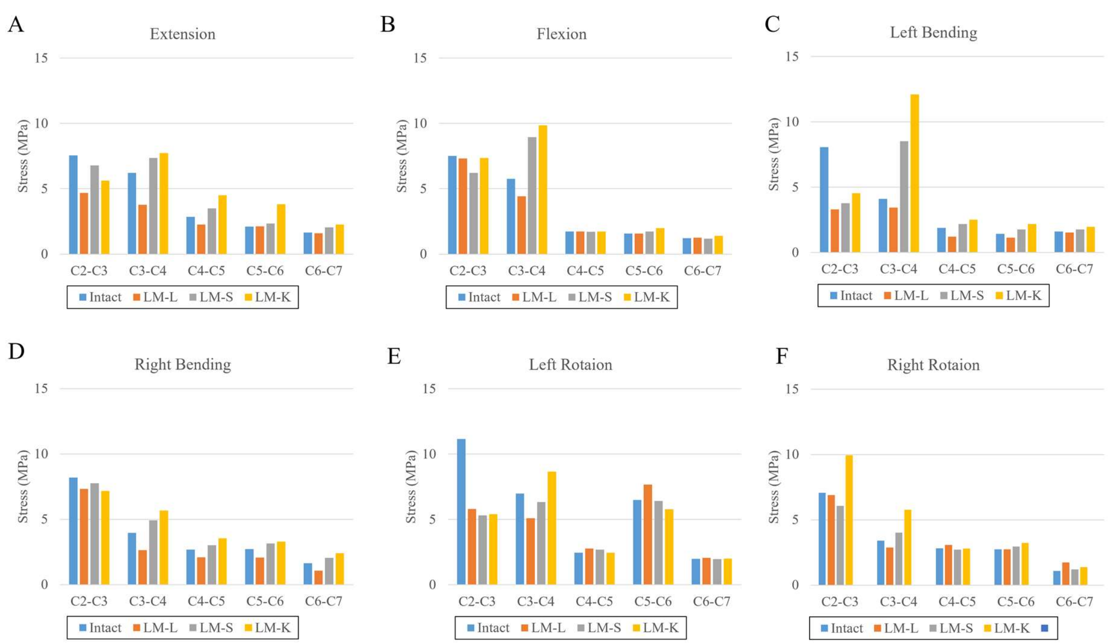

 doi:10.20944/preprints202203.0409.v1

Figure 4. Annulus Pressure. (a) extension, (b) flexion, (c) left bending, (d) right bending, (e) left rotation, and (f) right rotation. The vertical axis is stress (Mega Pascal; MPa), the horizontal axis is each intervertebral level.

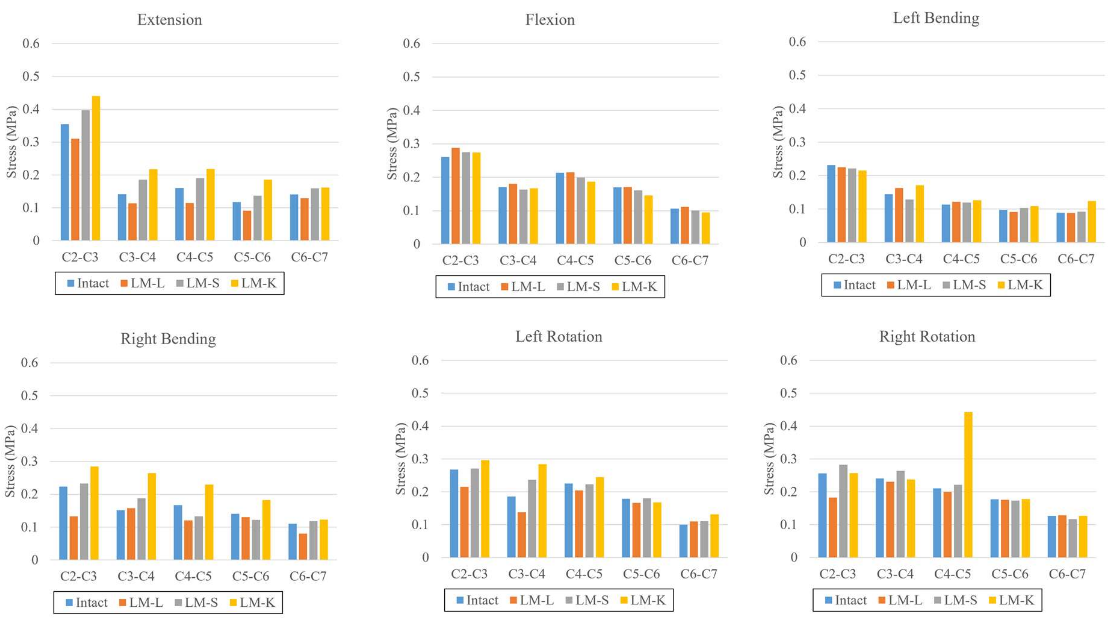

Figure 5. Nucleus stresses. (a) extension, (b) flexion, (c) left bending, (d) right bending, (e) left rotation, and (f) right rotation. The vertical axis is stress (MPa), the horizontal axis is each intervertebral level.

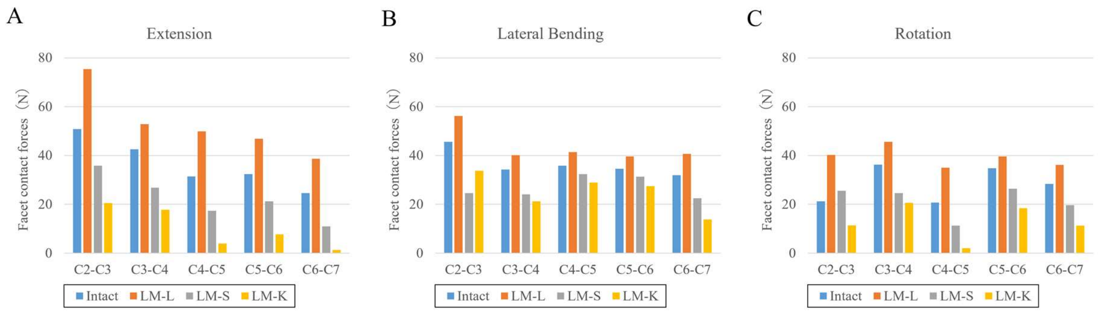

Figure 6. Facet contact forces. (a) extension, (b) lateral bending, (c) axial rotation. Vertical axis is force (N), horizontal axis is each intervertebral level.

Preprints (www.preprints.org) | NOT PEER-REVIEWED | Posted: 31 March 2022 doi:10.20944/preprints202203.0409.v1

TABLES

Table 1: Material properties assigned to the finite element model (14-16).

Component	Material Properties	Constitute Relation	Element Type	Area (mm^2)
Bone				
Vertebral cortical bone	E=10000 MPa v=0.3	Isotropic, Elastic	C3D8	-
Vertebral cancellous bone	E=450 MPa v=0.25	Isotropic, Elastic	C3D9	-
Vertebrae-Posterior	E=3500 MPa v= 0.25	Isotropic, Elastic	C3D10	-
Artificial bone	E=10000 MPa v= 0.3	Isotropic, Elastic	C3D8	-
Intervertebral Disc				
Ground substance of annulus fibrosis	C10=0.7 C01= 0.2	Hyper-elastic, Mooney-Rivlin	C3D8	-
Nucleus pulposus	C10=0.12 C01=0.03 D1=0	Incompressible Hyper-elastic, Mooney-Rivlin	C3D8	-
Ligaments				
Anterior Longitudinal Ligament	15.0(<12%),30.0(>12%) v= 0.3	Non-linear, Hypoelastic	T3D2	6.1
Posterior Longitudinal Ligament	10.0(<12%),20.0(>12%) v=0.3	Non-linear, Hypoelastic	T3D3	5.4
Capsular Ligament	7.0(<30%), 30(>12%) v=0.3	Non-linear, Hypoelastic	T3D4	46.6
Ligamentum Flavum	5.0(<25%), 10.0(>25%) v=0.3	Non-linear, Hypoelastic	T3D5	50.1
Interspinous Ligament	4.0(20-40%),8.0(>40%) v=0.3	Non-linear, Hypoelastic	T3D6	13.1
Facet Joints				
Apophyseal Joints	Non-linear Soft contact, GAPPUNI elements	-	-	-